Structural, electronic and energetic properties of uranium–americium mixed oxides $U_{1-y}Am_yO_2$ using DFT+U calculations

Martin S. Talla Noutack, Gérald Jomard, Michel Freyss, Grégory Geneste

HAL Id: cea-02535457
https://cea.hal.science/cea-02535457

Submitted on 2 Feb 2022

Structural, electronic and energetic properties of uranium–americium mixed oxides $U_{1-y}Am_yO_2$ using DFT+U calculations

Martin S. Talla Noutack[1] ⓘ **, Gérald Jomard**[1]**, Michel Freyss**[1,3] **and Grégory Geneste**[2]

[1] CEA, DEN, DEC, Cadarache, F-13108 Saint-Paul-Lez-Durance, France
[2] CEA, DAM, DIF, F-91297 Arpajon, France

Abstract

In this paper, we determine for the first time the electronic, structural and energetic properties of $U_{1-y}Am_yO_2$ mixed oxides in the entire range of Am content using the generalized gradient approximation (GGA)+U in combination with the special quasirandom structure (SQS) approach to reproduce chemical disorder. This study reveals that in $U_{1-y}Am_yO_2$ oxides, Am cations act as electron acceptors, whereas U cations act as electron donors showing a fundamental difference with $U_{1-y}Pu_yO_2$ or $U_{1-y}Ce_yO_2$ in which there is no cation valence change in stoichiometric conditions compared to the pure oxides. We show for the first time that the lattice parameter of stoichiometric $U_{1-y}Am_yO_2$ follows a linear evolution which is the structural signature of an ideal solid solution behavior. Finally, using two approaches (SQS and parametric), we show by assessing the enthalpy of mixing that there is no phase separation in the whole range of Am concentration.

Keywords: DFT + U, special quasirandom structure, mixed oxides, uranium, americium

1. Introduction

Actinides compounds exhibit many complex properties and also attract much interest for their industrial applications. Especially, americium-bearing oxides exhibit peculiar properties such as high oxygen potential [1, 2] and are submitted to significant self-irradiation effects. Furthermore, mixed uranium–plutonium oxides envisaged as the fuel for fast neutron reactors will be fabricated from spent uranium oxide fuel and will, as a consequence contain a few percent of americium. Therefore, one of the current nuclear challenge for technolgical application of americium-bearing oxides is to know whether the presence of americium will affect properties of fast neutron nuclear fuels. The understanding of the microstructure evolution of oxide fuels as well as their thermodynamic properties as a function of their composition constitute an important step towards their qualification for technolgical nuclear applications.

Although the density functional theory (DFT) within the local density approximation or generalized gradient approximation (GGA) is widely used for a large panel of compounds, its applicability for actinides oxides fails because of the complex features of the *5f* electrons, which require dedicated treatments. In fact, the traditional exchange-correlation functionals (GGA or LDA) do not capture the strong correlation effects relation to the localization of the *f* electrons. DFT+U is one of the state-of-the art approaches extensively and successfully used for correlated materials.

Moreover, the $U_{1-y}Am_yO_2$ solid solution displays a chemical disorder in the cationic sublattice i.e. cations

[3] Author to whom all correspondence should be addressed.

randomly occupy a face-centered-cubic (fcc) lattice and as a consequence, a very accurate modelling requires a very large supercell (several thousand atoms) for a good description of the chemical disorder. Since first-principles calculations are currently limited to a few hundred atom supercells especially for actinides oxides, the cationic distribution in the fcc lattice, which better reproduces the chemical disorder, needs to be approximated. As a first approximation, the U and Am cations can be distributed randomly in the fcc lattice (for a given composition), and a configurational average energy and other properties can be calculated. However, owing to the high computing time (enhanced in actinides coupounds) and given the large number of configurations for a large supercell, such an approach appears impractical. In order to overcome this shortcoming posed by cationic disorder in solid solutions using first-principles calculations, several approaches have been developed. One of them is based on special quasirandom structures (SQS) developed by Zunger *et al*. [3]. The SQS method has been shown to be relevant for transition element alloys [4] and uranium–plutonium mixed oxides [5].

The structural and electronic properties of $U_{1-y}Am_yO_2$ solid solutions have been the subject of very few experimental investigations in literature. For instance, Mayer *et al*. [6] examined the electronic structure of (U,Am)O$_2$ mixed oxide using x-ray photoemission spectra (XPS). More recently, the electronic and structural properties of these oxides have been analysed using extended x-ray absorption near edge (XANES) and extended x-ray absorption fine structure (EXAFS) [1, 2, 7] as well as x-ray diffraction (XRD) [8] experiments. Despite these investigations, the knowledge of many properties remains limited. For example, the early experiments show a discrepancy regarding the lattice constant as a function of Am content. This can be attributed to the self-irradiation effects which is known to occur in the Am-bearing oxides. In addition, literature does not provide any data on the mixing enthalpy which is one of the quantity required to conclude on the structural stability of the random alloys. Concerning cation electronic valences in $U_{1-y}Am_yO_2$ solid solutions, all available experimental studies do not agree with each other. Thus, DFT+U calculations in combination with the SQS approach are expected to support the available experimental results and, moreover, predict some missing data.

The present study reports results on the structural, electronic and energetic properties of $U_{1-y}Am_yO_2$ in the framework of DFT+U calculations. In section 2, we present the computational details. In section 3, electronic properties are presented and discussed. In section 4, the local crystallographic structure and lattice parameter are investigated. Finally, we present in section 5 energetic properties.

2. Computational scheme

2.1. DFT+U method

Our DFT calculations are carried out using the ABINIT package [9] (version 8.8.2). We use the projector augmented wave (PAW) [10, 11] formalism which is particularly efficient for the description of complex phases in which atomic relaxations are important.

The exchange and correlation effects are described by the GGA parameterized by Perdew *et al*. [12]. In order to take into account the strong correlations among *5f* electrons, an additional onsite Coulomb repulsion is considered by including a Hubbard-like term in the Hamiltonian [13]. The rotationally invariant form by Liechtenstein *et al*. [14] is used for the electron interaction energy related to the Hubbard term (E_{Hub}). The total energy is the sum of GGA energy (E^{GGA}) for a given density, the Hubbard interaction energy E_{Hub} and the double counting term E_{dc}:

$$E^{GGA+U} = E^{GGA} + E_{Hub} - E_{dc}. \tag{1}$$

The last two terms depend on the occupation matrix of the correlated orbitals.

For the double counting expression, we have chosen the 'full localized limit' (FLL) [13, 14] because the ground state of americium oxides is insulating and thus, *5f* orbital occupation is close to one or zero.

The onsite Coulomb terms U and J are set in the mixed oxides to the same values as for the end members i.e. (U ; J) = (4.50; 0.54) eV for UO$_2$ and (6.00 ; 0.75) eV for AmO$_2$ [15]. This assumption has been already made for (U,Pu)O$_2$ [5] to successfully compute bulk properties. Note that, in our previous study [16], by computing several bulk properties of AmO$_2$ as a function of the U and J parameters and comparing with the available experimental data, we showed that ($U = 6.00; J = 0.75$) eV values can be used to provide a good description of AmO$_2$.

In order to search the ground state within the DFT+U method, we applied the occupation matrix control scheme [17, 18] on the *5f* orbitals. In UO$_2$, a given U^{4+} ion has two *5f* electrons and in AmO$_2$ a given Am^{4+} ion has five *5f* electrons. Therefore, there are 21 possible diagonal matrices for UO$_2$ and AmO$_2$ referring to different manners to fill the seven *5f* orbitals of a given spin channel with two electrons (UO$_2$) or five electrons (AmO$_2$), thus 21 × 21 electronic configurations for $U_{1-y}Am_yO_2$ assuming (i) U^{4+} and Am^{4+} in high-spin electronic configuration and (ii) that the occupation matrix is the same for all the atoms of a given chemical species in the supercell. Given the large number of electronic configurations and high computational time, the systematic exploration of these 21 × 21 occupation matrices is very complex. Moreover, as we will see later, some of the U and Am atoms in the mixed oxide may undergo a change of their oxidation state, involving therefore a change of their occupation matrix, which complexifies the problem. As a starting point for searching the ground-state of the mixed oxides, *5f* occupation matrices orbitals of the end members UO$_2$ and AmO$_2$ (taking into account their valence states) can be applied, allowing to control possible electronic charge tranfers which induces change in the atomic valence states.

Note that the modelling of $U_{1-y}Am_yO_2$ mixed oxide required a rigorous methodology. Indeed, in order to model the electronic charge transfer occurring during calculations, we have first to suppress all symmetries to prevent charges (electrons or holes) to remain delocalized over the supercell. First, preliminary calculations show that some charge tranfers

spontaneously take place in the supercell and may lead to the formation of Am^{3+} and U^{5+}. The atoms undergoing this change of their valence state are thus spotted. However this preliminary step is not sufficient to maintain completely hole localized on a single U atom. Holes can only be completely localized (instead of being delocalized throughout the supercell) in the presence of an initial sufficient distortion around the U atoms. We thus proceed in two main steps:

(i) Obtain a distortion field by constraining the charge state of the atoms according to the preliminary step mentioned above: this is done by maintaining the *5f* occupation matrices constant (each matrix being related to the valence state of the corresponding cation) along the 20 to 30 first steps of all the self-consistent cycles of this pre-optimization. The aim is to first create the distortion needed to have the charge transfer and then leave the system converge to the correct final state. This pre-optimization step is performed until the complete localization of the holes on the U^{4+} cations.

(ii) Final structural optimization without constraint: the system is completely optimized without any constraint, starting from the last geometry and previous occupation matrices, but which are kept fixed only on the 20–30 first steps of the first self-consistent cycle.

The 1k antiferromagnetic (AFM) state is generally used as an approximation of the 3k AFM order in UO_2 [19] and AmO_2 [16]. Thus, the magnetic state of mixed uranium–americium oxide is assumed here to be a 1k AFM order.

2.2. Special quasirandom (SQS) approach

The SQS method is a randomness lattice theory consisted in mimicking as closely as possible the spatial correlation functions of an infinite random alloy within a finite size supercell [3]. This theory is based on the minimisation of the error function denoted $\epsilon(\sigma)$ (given in equation (2)) which corresponds to the averaged difference between the spatial correlation functions of a given structure σ (at any order) and the spatial correlation functions of an infinite random solid solution (which are known theoretically).

$$\epsilon(\sigma) = \sum_f \frac{D_f}{(k\bar{d}_f)^n} \left| \bar{\Pi}_f(\sigma) - \langle \bar{\Pi}_f \rangle_R \right|. \quad (2)$$

In this equation, the atomic lattice is discretized into its component figures $f = (k, m)$ where k is the number of vertices or sites and m is the maximum number of neighbour distances. D_f is the symmetry defined multiplicity of a figure and $\bar{\Pi}_f(\sigma)$ (for a given $f = (k, m)$) is defined in [3] as the average over the lattice sites (and possible orientations) of the spin products (the spin of a site is either $+1$ or -1 according to the chemical species on that site) of the k atoms placed at a maximal distance m from each other, and $\bar{d}_f$ is the mean distance between two given sites in a figure f. Based on the equation (2), von Pezold *et al.* [20] proposed the atomic fractional coordinates of SQS structures of 32-atom fcc supercells of binary A–B alloys for all atomic composition and in increments of 2/32. For more
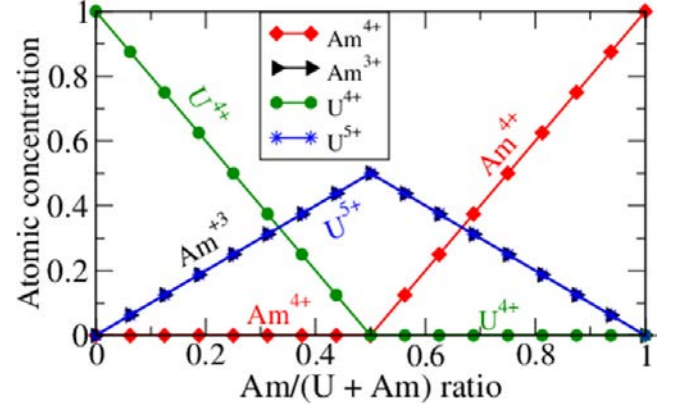

Figure 1. Concentration of the cationic species in the crystal as a function of the americium content.

details about the SQS approach see [3, 20]. We have used the configurations given by von Pezold *et al.* [20].

2.3. Computational parameters

Results are obtained using a plane-wave cutoff energy equal to 871 eV with the ABINIT code. According to our convergence tests, this input parameter lead to a precision lower than 1 meV per atom on physical energies (energy difference). 96-atom supercells ($2 \times 2 \times 2$) are used. The calculations are done on a $2 \times 2 \times 2$ *k*-points mesh generated by the Monkhorst–Pack [21] method, which is sufficient for an energy convergence less than 0.3 meV per atom. We performed full relaxation of the cell until the pressure acting on the system becomes lower than 5×10^{-7} Ha $Bohr^{-3}$ ($\sim$0.15 kbar) and on forces, for the structural optimization, less than $5 \cdot 10^{-4}$ Ha $Bohr^{-1}$ ($\sim$0.025 eV Å^{-1}).

3. Electronic properties

In this section, we study the electronic structure and the valence state of cations (U,Am) in the mixed oxides. The knowledge of the valence state of ions in a compound is required to compute its phase diagram. In particular, the thermodynamic computational method CALPHAD [22] uses a sublattice model based on the information on the valence state of species [23]. Furthermore, the knowledge of the cations valence state and electronic structure are needed to subsequently model atomic transport properties, which control the microstructure evolution of materials.

3.1. Valence state of (U,Am) in mixed oxides

3.1.1. (a) Stoichiometric conditions. We investigate the oxidation state of Am and U cations in the $U_{1-y}Am_yO_2$ mixed oxides in the stoichiometric conditions (i.e. O/(U + Am) =2) as a function of the Am content in the whole range of Am concentration. Figure 1 in addition to table 1 shows the evolution of the cationic species concentration. Depending on the Am content, two different behaviors are observed.

Table 1. Valence states of cations (Am,U) in $U_{1-y}Am_yO_2$ mixed oxides. The total Am atomic fraction (y) as well as the atomic fractions of all cations in the crystal are displayed. O/M (M $= U +$ Am) is the oxygen/metal ratio. For comparison, the results from the XANES experiments are also displayed.

		Atomic fraction (% at.)					
		y	Am(+III)	Am(+IV)	U(+IV)	U(+V)	O/M
		6.25	6.25	0.00	87.50	6.25	2
%Am < 50		18.75	18.75	0.00	62.50	18.75	2
	Exp. [2]	15.00	15.00	0.00	71.00	14.00	2
%Am > 50		68.75	31.25	37.50	0.00	31.25	2

Table 2. Valence state of cations (Am,U) in mixed oxides. The total Am atomic fraction (y) as well as the atomic fractions of all cations in the crystal are displayed. O/M is the oxygen/metal ratio. For comparison, the result on $(U,Pu)O_2$ mixed oxides from the XANES experiments [25] is also displayed.

		$U_{1-y}Am_yO_{2-x}$			
		Atomic fraction (% at.)			
y	Am(+III)	Am(+IV)	U(+IV)	U(+V)	O/M
6.25	6.25	0.00	93.75	0.00	1.97
		$U_{1-y}Pu_yO_{2-x}$ [25]			
		Atomic fraction (%)			
y	Pu(+III)	Pu(+IV)	U(+IV)	U(+V)	O/M
30.00	4.00	26.00	70.00	0.00	1.98

From 0% to 50%, one can see that Am(+IV) cations are all reduced to Am(+III) whereas uranium cations have mixed valence (+IV/+ V) with the U(+V) content equals that of Am. We highlight that the U(+V) cations are located close as possible to the Am(+III) cations i.e. in the first or second coordination shell depending on the possibility offered by the SQS configuration. We can conclude that U(+V) accommodate the formation of Am(+III). These results are the first theoretical confirmation of the XANES experiments (see [6, 8, 24]). Indeed, these experimental studies (limited to Am content lower than 20%) show by analysing the XANES spectra that U cations have mixed valence states (+IV/+ V) in $U_{1-y}Am_yO_2$ where americium cations are trivalent. In summary, all the Am(+IV) cations are reduced to Am(+III) when there are sufficient U(+IV) to be oxidized in U(+V) in order to accommodate charge neutrality and the formation of Am(+III).

On the contrary, for Am/(Am + U) > 50%, literature does not provide any investigation thus, the present study is a prediction regarding the valence state of the cations. Our DFT+U results show that (see table 1, %Am >50), contrary to the Am content less than 50%, U cations are now completely oxidized in U(+V) whereas Am cations are found in mixed valence (+III/+ IV). Moreover, figure 1 shows a change of behavior at Am/(Am + U) ratio equals to 50%. This point corresponds to the maximun concentration of trivalent americium and pentavalent uranium.

The valence state of cations in $(U,Am)O_2$ shows a significant difference with other mixed oxides like $(U,Pu)O_2$ or $(U,Ce)O_2$ for which the valence state of cations in stoichiometric conditions remains +IV. In other words, mixing U and Am oxides leads to a chemical oxidoreduction reaction which is not the case with $(U,Pu)O_2$ or $(U,Ce)O_2$.

3.1.2. (b) Hypo-stoichiometric conditions. We have also investigated the valence state of Am and U cations in mixed oxides for hypo-stoichiometric conditions. In order to induce hypo-stoichiometric conditions, a neutral oxygen vacancy is created in a 96-atom supercell. Table 2 displays the valence state of cations obtained in hypo-stoichiometric conditions as well as the results for $U_{1-y}Pu_yO_2$ from XANES experiments [25]. Note that for Am/(U + Am) =6.25%, there is three possible initial chemical environments (containing U and/or Am atoms) around an oxygen vacancy. The tetrahedron formed by: (i) two Am and two U cations, (ii) one Am and three U cations and (iii) four U. For these three configurations around the oxygen vacancy we have the same description of the valence state of cations in the supercell as displayed in table 2. We highlight, however, that the energetically most favourable configuration is the one including two Am in the first coordination shell i.e. the configuration (i).

Because of the lack of other studies on $(U,Am)O_2$ in hypo-stoichiometric conditions, only the results of $U_{0.7}Pu_{0.3}O_{2-x}$ from XANES experiments by Vigier *et al.* [25] have been displayed for comparison. Knowing that hypo-stoichiometry in UO_{2-x} is accommodated by the reduction of U(+IV) to U(+III), one could expect to have the same behavior in $U_{1-y}Am_yO_{2-x}$ mixed oxides. However, we can see from table 2 that the hypo-stoichiometry in $U_{1-y}Am_yO_{2-x}$ is rather accommodated by the reduction of U(+V) to U(+IV) since the U cations have mixed valence states (+IV and +V) in the perfect $U_{1-y}Am_yO_2$ compounds. Actually a neutral oxygen

Table 3. Valence state of cations (Am,U) in mixed oxides in the presence of a charged oxygen vacancy. The total Am atomic fraction (y) as well as the atomic fractions of all cations in the crystal are displayed. O/M is the oxygen/metal ratio. For comparison, the results of the perfect supercell are also plotted.

			$U_{1-y}Am_yO_{2-x}$			
			Atomic fraction (% at.)			
	y	Am(+III)	Am(+IV)	U(+IV)	U(+V)	O/M
$q = +1$	6.250	6.250	0.000	90.625	3.125	1.970
$q = +2$	6.250	6.250	0.000	87.500	6.250	1.970
			$U_{1-y}Am_yO_2$			
			Atomic fraction (% at.)			
	y	Am(+III)	Am(+IV)	U(+IV)	U(+V)	O/M
Perfect	6.250	6.250	0.000	87.500	6.250	2.000

vacancy releases two electrons, therefore driving to the reduction of two U(+V) cations to two U(+IV) cations.

We thus confirm that in $U_{1-y}Am_yO_2$ there is a charge transfer from U(+IV) to Am(+IV), which explains the formation of U(+V) and Am(+III) in equal concentration in the stoichiometric conditions. This result shows a difference with $(U,Pu)O_2$ in which the hypo-stoichiometry is accommodated by the reduction of Pu(+IV) to Pu(+III) (see table 2).

The electrons released by the neutral oxygen vacancy can diffuse throughout the crystal instead of localizing on a single atom in the vinicity of the vacancy leaving behind a partially ionized $V_O^\bullet$ ($q = +1$) or completely ionized $V_O^{\bullet\bullet}$ ($q = +2$) vacancies. When an ionized oxygen vacancy ($q = +2$ for example) is induced in $U_{1-y}Am_yO_2$ as diplayed in table 3, the valence state of cations is identical to what is observed in perfect $U_{1-y}Am_yO_2$.

In order to enlight the mechanism of electronic charge transfer occuring in $(U,Am)O_2$ solid solution, it is important to investigate the electronic structure.

3.2. Electronic structure

To understand the electronic structure of $U_{1-y}Am_yO_2$ mixed oxides and compare it to UO_2 oxide, the density of states (DOS) of the former were calculated and are illustrated in figure 2. The top of the valence band was set as the reference energy.

We observe in figure 2 that the band gap of $U_{1-y}Am_yO_2$ is formed between the U f components (U(+IV) and U(+V)) confirming that U(+IV) is partially oxidized to U(+V) in the solid solution. It is known that the band gap of AmO_2 is formed between the Am f and O p components [26] such that charge is prone to be transferred from O p to Am f components, whereas the gap of UO_2 is formed between the U f components (see figure 2). In addition, the band gap of AmO_2 is smaller than the UO_2 one, which is 2 eV. These results indicate that the reduction of Am(+IV) to Am(+III) according to the $Am^{4+} + 1/2O^{2-} \longrightarrow Am^{3+} + 1/4O_2$ equation is more favourable than the reduction of U(+IV) to U(+III) according to the $U^{4+} + 1/2O^{2-} \longrightarrow U^{3+} + 1/4O_2$ equation. The high oxygen potential of AmO_2 compared to that of UO_2 could account for this difference.
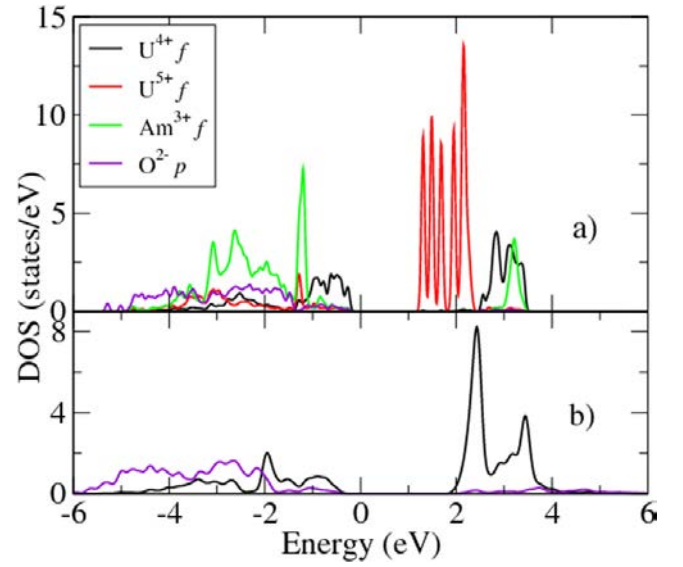

Figure 2. The DOS of Am^{4+}-f, Am^{3+}-f, U^{4+}-f, U^{5+}-f and O-p components in (a) $U_{1-y}Am_yO_2$ (with $y = 6.25\%$) and (b) UO_2 computed by DFT+U. The density given here is the projected density on a given atom.

The partial oxidation of U(+IV) to U(+V) might be explained as follow: Am acts as an electron acceptor and U is an electron donor (according to the $U^{4+} + 1/4O_2 \longrightarrow U^{5+} + 1/2O^{2-}$ equation) in the solid solution of the $(U,Am)O_2$ mixed oxide. Thus, the chemical reaction related to this mechanism can be written as $Am^{4+} + U^{4+} \longrightarrow Am^{3+} + U^{5+}$. Such a mechanism has been previously observed in $U_{1-y}Pu_yO_{2\pm x}$ solid solution but only in hypo-stoichiometric conditions using electrical conductivity measurements, where a charge tranfer reaction $Pu^{4+} + U^{4+} \longrightarrow Pu^{3+} + U^{5+}$ was suggested [27].

4. Structural properties

In this section, we investigate structural properties of $U_{1-y}Am_yO_2$ namely the lattice parameter as well as the interatomic distances (in the first cordination shell) as a function of Am content Am/(Am + U) in the 0%–100% range.

Table 4. Lattice parameters of $U_{1-y}Am_yO_2$ mixed oxides in the whole Am concentration range.

y (% at.)	0.00	6.25	12.50	18.75	25.00	31.25	50.00	68.75	75.00	93.75	100.00
a (Å)	5.540	5.533	5.527	5.520	5.518	5.511	5.505	5.474	5.469	5.443	5.438
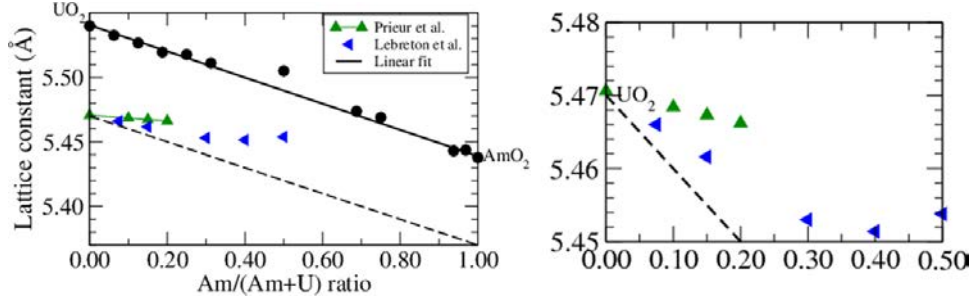
Figure 3. Lattice parameter of $U_{1-y}Am_yO_2$ computed by DFT+U compared to the experimental data. The black circles represent the calculated values fitted by a linear expression (black line), the diamonds (blue and green) are the XRD experiments and the dotted line is the evolution of the lattice parameter obtained by a linear combination of the UO_2 and AmO_2 lattice parameters. On the left, we zoomed the experimental data over the 0% to 50% Am concentration range.

4.1. Lattice parameter

Assuming a linear behavior of lattice parameter as a function of composition in mixed oxides, Kato *et al.* [28] proposed an analytical expression based on the experimental ionic radius of the species in the pure compounds and taking deviation from stoichiometry into account. For instance, ionic radius of Am^{4+},U^{4+} and O^{2-} should be used for $U_{1-y}Am_yO_2$ mixed oxides. However, this analytical expression is not suitable for mixed $U_{1-y}Am_yO_2$ oxides because of various valence states of the species: Am^{3+}, Am^{4+}, U^{4+}, and U^{5+}. We thus calculate the lattice parameter in the whole range of Am concentration and results are reported in table 4.

In the figure 3, we display the lattice parameter as a function of Am content together with experimental results from XRD analysis [7, 24] for comparison. We also display the results obtained by a linear combination of the UO_2 and AmO_2 experimental lattice parameters (dotted lines) given by the following equation:

$$a_{U_{1-y}Am_yO_2} = (1-y)a_{UO_2} + ya_{AmO_2}. \quad (3)$$

One can clearly see that the calculated lattice parameter of $U_{1-y}Am_yO_2$ as a function of Am content follows a linear behavior (black line) expected for a stoichiometric ideal solid solution. We also observe that although our results (black line) show a slight overestimation ($\sim$1.3% which is in the error margin of the GGA+U method) compared to the dotted line which is yielded by linear combination of the experimental data, both lines have the same slope. Note that the change in cation valence does not have a significant effect on the evolution of the lattice parameter as a function of the composition. In other words, the evolution of the lattice parameter remains linear as in the case of $(U,Pu)O_2$ or $(U,Ce)O_2$ in which the valence states of cations do not change. The compensation mechanisms between U and Am cations could account for this behavior. While the reduction of Am (+IV) to Am (+III) is associated to an increase ($\sim$11.5%) in the ionic radius from 0.95 Å to 1.09 Å, the oxidation of U (+IV) to U

(+V) is associated to a decrease ($\sim$11.2%) in the ionic radius from 1.01 Å to 0.89 Å. One can also see that the experimental values (blue and green diamonds) are scattered. Lattice expansion under self-irradiation effects, which is known to occur in ^{241}Am-bearing oxides [29–31] can account for this discrepancy. Moreover, the evolution of the experimental values as a function of the Am content does not have the same slope as the lines from the linear combination of UO_2 AmO_2 lattice parameters (black and dotted lines) which is the behavior expected for a stoichiometric ideal solid solution.The deviation from stoichiometric (enhanced for %Am > 30) combined with the oxygen interstitials observed by Lebreton *et al.* [29] in the samples they characterized could account for this behavior. It would be interesting to further investigate in the framework of DFT+U the effect of point defects as well as cluster defects on the structural properties of $U_{1-y}Am_yO_2$ mixed oxides, especially on the lattice parameter in order to support the experimental studies. It will be investigated in the near future.

4.2. Interatomic distances

In order to provide a deeper understanding of the effect of the Am content on the atomic local environment of UO_2 oxide and more details on the structure of $U_{1-y}Am_yO_2$, interatomic distances are analysed and reported in table 5. We also reported in parenthesis the relative variation Δd of the interatomic distances with respect to the experimental (resp. calculated) distances in pure UO_2 defined as :

$$\Delta d = \left| \frac{d - d_{\text{ref}}}{d_{\text{ref}}} \right| \quad (4)$$

where d_{ref} is the U–O interatomic distance in the UO_2 pure oxide.

Though our DFT+U results show a slight overestimation (which is a well known tendency of the DFT+U method as stated previously) of bond lengths compared to the EXAFS results, one can see that our results are in good agreement with

Table 5. Interatomic distances of $U_{1-y}Am_yO_2$ in comparison with the EXAFS experiments [24]. In parenthesis are the relative variation Δd defined in equation (4). These distances are the avrage distance over the first coordination shell of a given specie with a statistical error 0.02 Å.

	y (%)	Distances (Å)			
		$d_{\mathrm{U-U}}$	$d_{\mathrm{U-Am}}$	$d_{\mathrm{U-O}}$	$d_{\mathrm{Am-O}}$
	0.00	3.89	/	2.40	/
	6.25	3.90	3.90	2.35(0.02)	2.47
	12.50	3.90	3.89	2.34(0.02)	2.47
Exp. [24]	15.00	3.86	3.87	2.33(0.02)	2.43

the experimental data by Prieur *et al.* [24]. In particular, the predicted variation of U–O distance equals to $\Delta d = \sim 2\%$ is very close to the measured one.

The bond length of the first oxygen atoms surrounding Am atoms is 2.47 ± 0.02 Å which is in agreement with that obtained for the Am(+III)–O distances in pure Am_2O_3.

The first U(+IV)–O distances (2.35 ± 0.02 Å) are slightly shorter than in UO_2 pure oxide (2.40 ± 0.02 Å) indicating the structural modification due to the presence of Am. The first U(+IV)–U(+IV) or U(+IV)–Am(+III) bond lengths are 3.90 ± 0.02 Å. The same bond length for both U(+IV)–U(+IV) and U(+IV)–Am(+III) indicates a random distribution in the cationic sublattice confirming the ideal solid solution behavior of $U_{1-y}Am_yO_2$ oxides.

5. Energetic properties

To evaluate the stability of alloyed compounds, the free enthalpy of mixing is usually considered [4, 5, 32]. The Gibbs free energy of mixing refers to the energy difference of a configurationally random alloy where the atomic species randomly occupy lattice positions [33] with respect to the pure compounds. The Gibbs free energy of mixing is given by:

$$\Delta G_{\mathrm{mix}} = \Delta H_{\mathrm{mix}} - T\Delta S_{\mathrm{mix}} \tag{5}$$

where ΔH_{mix} is the mixing enthalpy and ΔS_{mix} the mixing entropy. For the zero temperature, $\Delta G_{\mathrm{mix}} = \Delta H_{\mathrm{mix}}$.

The mixing enthalpy of $U_{1-y}Am_yO_2$ is defined as:

$$\Delta H_{\mathrm{mix}}(y) = H^{U_{1-y}Am_yO_2} - (1-y)H^{UO_2} - yH^{AmO_2}. \tag{6}$$

The mixing enthalpy is computed in the current study using both SQS configurations and a parametric approache introduced by Sluiter [32] and already used for $U_{1-y}Pu_yO_2$ [5]. The parametric approach is based on a polynomial representation of $\Delta H_{\mathrm{mix}}(y)$. Assuming a third-order cubic representation and using the limiting conditions $\Delta H_{\mathrm{mix}}(0) = \Delta H_{\mathrm{mix}}(1) = 0$ corresponding to the pure elements, it can be shown that:

$$\Delta H_{\mathrm{mix}}(y) = \Delta H_{\mathrm{sol}}^{\mathrm{U\ in\ AmO_2}} y^2(1-y) + \Delta H_{\mathrm{sol}}^{\mathrm{Am\ in\ UO_2}} y(1-y)^2 \tag{7}$$

where $\Delta H_{\mathrm{sol}}^{\mathrm{U\ in\ AmO_2}}$ and $\Delta H_{\mathrm{sol}}^{\mathrm{Am\ in\ UO_2}}$ are the solution enthalpies for uranium in the lattice of AmO_2 and vice versa respectively. Fore more details see Refs. [4, 5, 32].

The parametric approach has been successfully used in β-Ti with transition elements [4] and in $U_{1-y}Pu_yO_2$ mixed oxides [5].
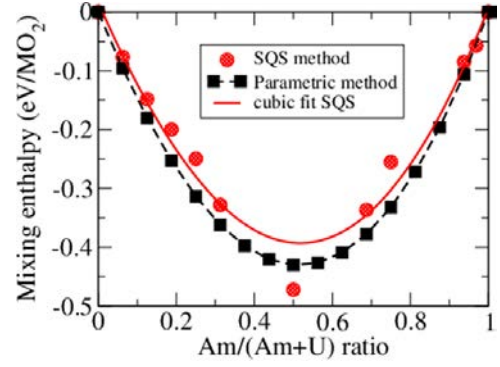

Figure 4. Solid solution mixing enthalpy $\Delta H_{\mathrm{mix}}^{\mathrm{SQS}}(y)$ and $\Delta H_{\mathrm{mix}}^{\mathrm{Par}}(y)$ of $U_{1-y}Am_yO_2$ calculated using the SQS configurations and the parametric approach.

Figure 4 shows $\Delta H_{\mathrm{mix}}^{\mathrm{SQS}}(y)$ and $\Delta H_{\mathrm{mix}}^{\mathrm{Par}}(y)$ over the whole range of composition. The enthalpy of mixing of UO_2 and AmO_2 is found negative in the entire range of Am concentrations whatever the method used indicating that there is no phase separation related to the variation of Am content. Furthermore, the points from the SQS approach fits well with the third-order polynomial shape (except the point corresponding to 50%). For a ratio Am/(Am + U) equal to 50%, the compound is more stable than all the other compositions. However, it is not excluded that it could be possible to find another configuration (SQS) with a mixing enthalpy closer to the cubic adjustment (red curve) than that shown in figure 4. Indeed, the configurations resulting from the SQS approach do not systematically lead to the lowest energy configuration but to the most disordered configuration. Note that the mixing enthalpy absolute values in $U_{1-y}Am_yO_2$ are about 100 times larger than the ones obtained in $U_{1-y}Pu_yO_2$ (using the same SQS configurations) [5] indicating the higher stability of mixed uranium–americium oxides compared to the mixed uranium–plutonium oxides.

$\Delta H_{\mathrm{mix}}^{\mathrm{Par}}(y)$ and $\Delta H_{\mathrm{mix}}^{\mathrm{SQS}}(y)$ show a good agreement with each other, with the maximum difference of not more than 40 meV per unit cell, validating the parametric approach for $U_{1-y}Am_yO_2$ solid solution.

These ΔH_{mix} results are the first prediction and are useful for the CALPHAD method for the computation of the phase diagram of the U–Am–O system since this phase diagram is not fully established.

6. Conclusion

The electronic structure, structural and energetic properties are computed in this study using the DFT+U calculations in combination with the SQS approach of structural disorder.

$U_{1-y}Am_yO_2$ mixed oxides show a particular valence state of cations which is fundamentally different from other mixed oxides like $U_{1-y}Pu_yO_2$ and $U_{1-y}Ce_yO_2$. Indeed, in $U_{1-y}Am_yO_2$, Am acts as an electron acceptor whereas U acts as an electron donor according to the $Am^{4+} + U^{4+} \longrightarrow Am^{3+} + U^{5+}$ mechanism. These results are in good agreement with early XANES experiments (limited to %Am < 20) but also

allow to complete them by providing a larger description of Am-bearing oxides over the entire range of Am content. We show that for %Am < 50, all Am(+IV) are reduced to Am(+III) whereas U has mixed valence (+IV and +V). On the contrary, when %Am > 50, Am(+IV) is partially reduced to Am(+III) whereas all U(+IV) cations are oxidized to U(+V). This study shows that the lattice parameter as a function of Am content follows a linear behavior that cannot be experimentally observed owing to the deviation from stoichiometry combined with the presence of oxygen interstitials (enhanced for the large Am content higher than 40%) observed in samples that have been experimentally charaterized in the early studies and subject to self irradiation. It would be interesting to further investigate in the framework of DFT+U the effect of point defects as well as cluster defects on the structural properties of $U_{1-y}Am_yO_2$ mixed oxides, especially on the lattice parameter. In addition, we show that U–Am and U–U bond lengths are identical which is the signature of the random distribution of cations in the cation sublattice. Thus, our study is the first confirmation of the ideal solid solution (from the structural point of view) behavior of $U_{1-y}Am_yO_2$ provided a perfect defectless and stoichiometric compound could be obtained. Using two approaches, (SQS and parametric), we show with satisfactory agreement between both approaches that there is no demixing in $U_{1-y}Am_yO_2$ in the whole range of Am at low temperature. This study is the first assessement of the mixing enthalpy of Am-bearing oxides, the minimum value being about $-0.45\,eV$.

The results obtained in this study support the experimental studies and, on the other hand, can be useful for thermodynamic computational methods like CALPHAD.

ORCID iDs

Martin S. Talla Noutack ● https://orcid.org/0000-0003-0249-1205

References

[1] Osaka M, Sato I, Namekawa T, Kurosaki K and Yamanaka S 2005 Oxygen potentials of $(U_{0.685}Pu_{0.270}Am_{0.045})O_{2-x}$ solid solution *J. Alloys Compd.* **397** 110–4

[2] Prieur D, Martin P M, Jankowiak A, Gavilan E, Scheinost A C, Herlet N, Dehaudt P and Blanchart P 2011 Local structure and charge distribution in mixed uranium–americium oxides: effects of oxygen potential and am content *Inorg. Chem.* **50** 12437–45

[3] Zunger A, Wei S-H, Ferreira L and Bernard J E 1990 Special quasirandom structures *Phys. Rev. Lett.* **65** 353

[4] Chandran M, Subramanian P and Gigliotti M F 2013 First principles calculation of mixing enthalpy of β-Ti with transition elements *J. Alloys Compd.* **550** 501–8

[5] Njifon I C, Bertolus M, Hayn R and Freyss M 2018 Electronic structure investigation of the bulk properties of uranium–plutonium mixed oxides (U,Pu)O2 *Inorg. Chem.* **57** 10974–83

[6] Mayer K, Kanellakopoulos B, Naegele J and Koch L 1994 On the valency state of americium in $U_{0.5}Am_{0.5}O_{2\pm x}$ *J. Alloys Compd.* **213** 456–9

[7] Lebreton F, Horlait D, Delahaye T and Blanchart P 2013 Fabrication and characterization of $U_{1-x}Am_xO_{2\pm\delta}$ compounds with high americium contents ($x = 0.3, 0.4$ and 0.5) *J. Nucl. Mater.* **439** 99–102

[8] Lebreton F, Horlait D, Caraballo R, Martin P M, Scheinost A C, Rossberg A, Jegou C and Delahaye T 2015 Peculiar behavior of (U,Am)$O_{2-\delta}$ compounds for high americium contents evidenced by XRD, XAS, and Raman spectroscopy *Inorg. Chem.* **54** 9749–60

[9] Gonze X *et al.* 2002 First-principles computation of material properties: the ABINIT software project *Comput. Mater. Sci.* **25** 478–92

[10] Kresse G and Joubert D 1999 From ultrasoft pseudopotentials to the projector augmented-wave method *Phys. Rev.* B **59** 1758

[11] Blöchl P E 1994 Projector augmented-wave method *Phys. Rev.* B **50** 17953

[12] Perdew J P, Burke K and Ernzerhof M 1996 Generalized gradient approximation made simple *Phys. Rev. Lett.* **77** 3865

[13] Anisimov V I, Zaanen J and Andersen O K 1991 Band theory and Mott insulators: Hubbard U instead of Stoner I *Phys. Rev.* B **44** 943

[14] Liechtenstein A I, Anisimov V I, Zaanen J and Andersen O K 1995 Density-functional theory and strong interactions: orbital ordering in Mott–Hubbard insulators *Phys. Rev.* B **52** R5467

[15] Kotani A and Ogasawara H 1993 Theory of core-level spectroscopy in actinide systems *Physica* B **186** 16–20

[16] Noutack M S T, Geneste G, Jomard G and Freyss M 2019 First-principles investigation of the bulk properties of americium dioxide and sesquioxides *Phys. Rev. Mater.* **3** 035001

[17] Dorado B, Jomard G, Freyss M and Bertolus M 2010 Stability of oxygen point defects in UO2 by first-principles DFT + U calculations: occupation matrix control and Jahn–Teller distortion *Phys. Rev.* B **82** 035114

[18] Jomard G, Amadon B, Bottin F and Torrent M 2008 Structural, thermodynamic, and electronic properties of plutonium oxides from first principles *Phys. Rev.* B **78** 075125

[19] Wilkins S, Caciuffo R, Detlefs C, Rebizant J, Colineau E, Wastin F and Lander G 2006 Direct observation of electric-quadrupolar order in UO2 *Phys. Rev.* B **73** 060406

[20] von Pezold J, Dick A, Friák M and Neugebauer J 2010 Generation and performance of special quasirandom structures for studying the elastic properties of random alloys: application to Al–Ti *Phys. Rev.* B **81** 094203

[21] Monkhorst H J and Pack J D 1976 Special points for brillouin-zone integrations *Phys. Rev.* B **13** 5188

[22] Sundman B, Lukas H and Fries S 2007 Computational thermodynamics: the Calphad method (New York: Cambridge University Press)

[23] Guéneau C, Dupin N, Sundman B, Martial C, Dumas J-C, Gossé S, Chatain S, De Bruycker F, Manara D and Konings R J 2011 Thermodynamic modelling of advanced oxide and carbide nuclear fuels: description of the U–Pu–O–C systems *J. Nucl. Mater.* **419** 145–67

[24] Prieur D, Lebreton F, Caisso M, Martin P, Scheinost A, Delahaye T and Manara D 2016 Melting behaviour of americium-doped uranium dioxide *J. Chem. Thermodyn.* **97** 244–52

[25] Vigier J-F, Martin P M, Martel L, Prieur D, Scheinost A C and Somers J 2015 Structural investigation of $(U_{0.7}Pu_{0.3})O_{2-x}$ mixed oxides *Inorg. Chem.* **54** 5358–65

[26] Suzuki C, Nishi T, Nakada M, Tsuru T, Akabori M, Hirata M and Kaji Y 2013 DFT study on the electronic structure and chemical state of americium in an (Am,U) mixed oxide *J. Phys. Chem. Solids* **74** 1769–74

[27] Fujino T, Yamashita T, Ohuchi K, Naito K and Tsuji T 1993 High temperature electrical conductivity and conduction mechanism of $(U,Pu)O_{2\pm x}$ at low oxygen partial pressures *J. Nucl. Mater.* **202** 154–62

[28] Kato M and Konashi K 2009 Lattice parameters of $(U,Pu,Am,Np)O_{2-x}$ *J. Nucl. Mater.* **385** 117–21

[29] Lebreton F, Belin R C, Delahaye T and Blanchart P 2012 *In situ* x-ray diffraction study of phase transformations in the Am–O system *J. Solid State Chem.* **196** 217–24

[30] Chikalla T and Eyring L 1968 Phase relationships in the americium-oxygen system *J. Inorg. Nucl. Chem.* **30** 133–45

[31] Prieur D, Martin P, Lebreton F, Delahaye T, Jankowiak A, Laval J-P, Scheinost A, Dehaudt P and Blanchart P 2012 Alpha self-irradiation effect on the local structure of the $U_{0.85}Am_{0.15}O_{2\pm x}$ solid solution *J. Solid State Chem.* **194** 206–11

[32] Sluiter M H and Kawazoe Y 2002 Prediction of the mixing enthalpy of alloys *Europhys. Lett.* **57** 526

[33] Sluiter M, Turchi P E A, Pinski F J and Stocks G M 1992 A first-principles study of phase stability in Ni–Al and Ni–Ti alloys *High Temperature Aluminides and Intermetallics* (Amsterdam: Elsevier) pp 1–8